A panchromatic modification of Metal-Organic Frameworks' light absorption spectra.

E. H. Otal,[a,b,] M. L. Kim, [a,b] M. E. Calvo, [d] L. Karvonen, [c] I. O. Fabregas, [b] C. A. Sierra, [e] and J. P. Hinestroza[f]

The optical absorption of UiO-66-NH$_2$ MOF was red-shifted using a diazo-coupling reaction. Modification done with naphtols and aniline yielded reddish samples and diphenylaniline yielded dark violet ones. The photocatalytic activity of modified MOFs was tested for Methylene Blue degradation, showing a good performance relative to TiO$_2$. Also the degradation performance is correlated to the red shift of absorption edge. These findings hint to potential applications in photocatalysis and in dye sensitized solar cells.

Metal-organic frameworks (MOFs) are coordination polymers with high surface area.[1] These supramolecular coordination complexes have rigid organic bridges linked to clusters of metal oxides coordinated through different groups like hydroxy, oxo, carboxylate, etc. The chemical and physical properties of MOFs can be tuned by a judicious selection of the linker, the metal-oxide centre and the pore size.

One of the most studied frameworks is MOF 5 [2], a MOF with a periodic arrangement of Zn$_4$O clusters as secondary building units (SBU) linked through terephthalate ions. This array of SBUs has a crystalline order that can be defined as a three-dimensional periodic pattern of II-VI semiconductor nanoparticles. However, unlike II-VI semiconductor nanoparticles prepared by chemical routes, where surface coordination and particle size distribution vary, in MOFs the number of atoms, coordination and distance in each Zn$_4$O cluster is crystallographically well defined.

MOFs can also behave as semiconductors.[3,4] The use of semiconductor nanoparticles in photocatalysis applications has the drawback of a potential reduction of the surface area due to the agglomeration of the nanoparticles. Additionally, their large band-gap energy leads mostly to absorption in the UV range of the electromagnetic spectrum. When MOFs are used, the first problem can be neglected due to the inherent high surface area of MOFs (>1000m^2/g), and the large number of highly accessible pores.

In semiconductors, the problem of shifting the absorption spectra to the visible range to improve the light harvesting of a semiconductor was solved by Grätzel et al.[5,6]. Their approach was based on the adsorption of a ruthenium complex dye at the surface of TiO$_2$ nanoparticles. This system opened a large new field in photovoltaics known as dye sensitized solar cells (DSSC). Recently, the use of a new family of metal-free dyes has allowed the replacement of ruthenium complexes in DSSCs.[7,8] These new systems are composed by an electron donor group (e.g. triphenylamine) bridged through a π-system (C=C or N=N) to an acceptor group (e.g. cyanoacrylic acid). Then, this Aceptor-π-Donor system (A-π-D) is attached to the semiconductor, typically TiO$_2$, through the carboxylic group.

This strategy can be also used to sensitize MOFs, by introducing different dyes as organic linkers, and thus, extending their spectral absorption to the visible range for the resulting material. One way to do so, include post-synthetic modifications of a synthon introduced as organic linker into the MOF structure. This strategy was early reported by Burrows et al. who used an aldehyde-synthon as linker on a Zn-based MOF for its later transformation into a hydrazone[9]. Similarly, nitrogen functional groups can be used, taking advantage of their chemical versatility which allow more flexibility than aldehydes in the reactions that can be performed. Jiang et al. performed a tandem diazotization reaction on MIL-101-Cr-NH$_2$ to introduce halo, hydroxyl and azo groups[10], Nasalevich et

a. *Laboratory for Materials Science and Technology, FRSC-UTN, Av. Inmigrantes 555, Río Gallegos 9400, Argentina.*
b. *Division of Porous Materials, UNIDEF, CITEDEF, CONICET, S.J.B de la Salle 4397, Villa Martelli (B1603ALO), Buenos Aires, Argentina.*
c. *Solid State Chemistry and Catalysis, Empa – Swiss Federal Laboratories for Materials Science and Technology, Überlandstrasse 129, CH-8600 Dübendorf, Switzerland.*
d. *Instituto de Ciencia de Materiales de Sevilla (Consejo Superior de Investigaciones Científicas-Universidad de Sevilla), C/Américo Vespucio 49, 41092 Sevilla, Spain.*
e. *Department of Chemistry, Faculty of Sciences, Universidad Nacional de Colombia, Bogotá, Colombia*
f. *Laboratory of Textiles and Nanotechnology, Department of Fiber Science and Apparel Design, Cornell University, Ithaca, New York*
Electronic Supplementary Information (ESI) available: Synthesis description, characterization details, photographs of powders, schemes of MOFs and TGA calculations. See DOI: 10.1039/x0xx00000x

al. who performed a diazo coupling to increase the visible light absorption range and improve the photocatalytic performance on MIL-125(Ti)-NH_2[11], and Aguilera-Sigalat and Bradshaw who modified UiO-66-NH_2 for fluorescent based pH sensors[12]. In our case, like in the last example, we use UiO-66-NH_2, a Zr-based MOF where the SBU is $Zr_6O_4(OH)_4$, enabling an exceptional stability in water [13, 14]. This enhanced water stability allows us to generate materials for photocatalytic applications in different environments and targets.

The diazo coupling reactions of UiO-66-NH_2 with N,N-dimethylaniline, 1-naphtol, 2-naphtol and diphenylamine yielded strongly coloured solids. Diazo coupling was not successful under the experimental conditions reported here when cresile blue, basic fuchsine, malachite green, or crystal violet were used. The failure of the reaction with these compounds was presumably due to the similar size of the molecules to the pore size of the MOF, both around 1nm. The coupling of these molecules with the amino groups closer to the external surface may also block the reactant access to the inner pores preventing their diffusion through the porous network to react with more internal amino groups. No diazo coupling was achieved when UiO-66 was testes as starting material.

In order to analyse the structural changes after the diazo coupling and concerning the crystallinity, we show in Fig. 1 the XRD diffraction patterns for all diazo coupled MOF powders. For the sake of comparison, all diffractograms were normalized to the (111) peak. In all cases, the samples exhibit the UiO-66 diffraction pattern with no extra phases but with differences in the intensity of some of the peaks. The differences are attributed to the introduction of rigid (but not static) organic groups that change the electronic density in certain planes of the UiO-66 crystalline structure. The most remarkable of these differences is observed in the (600) reflection that corresponds to a plane where the diazo group and part of the rigid organic chain are located. Also the intensity ratio of peaks (331)/(420) shows some variation. In UiO-66-NH_2, these two peaks exhibit a similar intensity but in the rest of the samples, the (331) reflection is more intense. The reason of this asymmetry is that the plane (331) crosses the aromatic rings of the terephthalate linkers across Carbon-2 and Carbon-5, where the amino group is attached, hence increasing the electronic density in the post-functionalized solids. In the second case, plane (420) crosses the terephthalate by a specular plane that does not include any carbon from the aromatic ring, hence keeping a constant electronic density when functionalization is performed (see ESI).
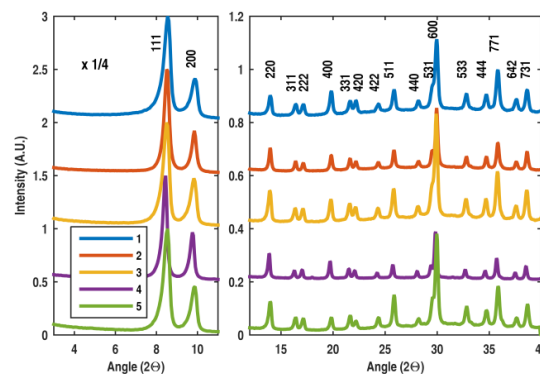

Fig 1 – X-Ray diffraction patterns for samples with and without diazo coupling reaction, left side reflection intensities divided by four. Samples ID: 1)UiO-66-NH_2 (blue line), 2) N,N-dimethylaniline (red line), 3) 1-naphtol (yellow line), 4) 2-naphtol (violet line), 5) Diphenylamine (green line).

To obtain information of the specific surface area in the modified MOFs, nitrogen sorption measurements were performed (See ESI). All isotherms exhibited type I behaviour, in agreement with previous reports for UiO-66.[15] Type I isotherms indicate microporous powders with a pore diameter size in the range of a few molecular nitrogen diameters. From these data we can estimate the specific surface area (SSA) for all the solids (Table 1). All samples exhibited a low SSA respect to those previously reported in bibliography (~1400m2/g)[16]. This observation can be assigned to the sensibility of the SSA to the synthesis conditions. Interestingly, the N,N-dimethylaniline coupled sample exhibited a higher SSA than the uncoupled one. This lack of correlation of SSA with the coupled organic side chain volume was previously observed in functionalized samples via amide formation with different acid anhydrides[17].

In order to analyse the solvent content, the approximate diazo coupling yield, and the average molar mass, a thermogravimetric analysis coupled to mass spectrometry (TGA-MS) of all the samples was performed. From the analysis of these results, we detected a first mass loss step attributed to water occluded in the pores, as shown by the m/s=18 peak (See ESI). The CO_2 peak (m/s=44) was not observed up to 450°C in the UiO-66 sample; while the rest of the samples exhibited a CO_2 signal around 350°C. The diphenylamine sample showed a complex decomposition path and its CO_2 peak appeared at 250°C. Even though diazo coupled samples have a high thermal stability, the structure modification made them less stable than the unmodified UiO-66.

The yield of the diazo coupling was roughly estimated from TGA-MS mass loss measurements. This estimation is based on the hypothesis that the mass losses correspond to the solvent elimination and transformation of the organic part of the MOFs to combustion products and ZrO_2. Also we speculate that the molecular mass of this organic part is composed by successfully diazo-coupled MOF and UiO-66-OH (product of diazonium salt decomposition). The values for a yield percentage of the diazo coupling reaction and a more detailed discussion are presented in the ESI. In all cases the yield of the diazo coupling was estimated

below 25%, similar yields were obtained for functionalization via amide formation[17]. This fact could be explained considering that the reactants diffuse through the pore, they may find several diazonium ion groups (the nucleophilic reaction has high efficiency, as N_2 is an excellent leaving group), and the coupling reaction will occur, making the reaction more likely on the sites closest to the surface. Once the coupling reaction occurs, the pore size is reduced, hence decreasing diffusion through the pores. As a consequence, an unreacted core and a shell of functionalized MOF are formed. The molecules that failed to react (cresile blue, basic fuchsine, malachite green and crystal violet) are drastic cases of surface pore blocking, shielding the internal part of the MOF and impeding the reaction to continue.

Raman spectroscopy was used to determine the tautomeric configuration of modified likers. Tautomeric equilibrium is related to the proton transfer among two or more functional groups in a molecule with direct impact in the electronic density and consequently, in the absorption spectra. In the case of modified MOFs, this equilibrium can be present and can be strongly influenced by temperature, solvent polarity, pH and electron withdrawing substituents[18]. Vibrational spectroscopies are a very precise tool to identify the predominant species in this tautomeric equilibrium. In the case of Infrared spectroscopy (FTIR) only the disappearance of amino groups in modified samples was clearly observed (See ESI). While Raman spectroscopy showed that samples coupled with N,N-dimethylaniline and diphenylamine are protonated and the azo-quinonoid equilibrium is displaced to the quinonoid-form due to the use of acetic acid and acetone during the washing step of the samples. The use of a polar solvent and an acid shifts the equilibrium to the quinonoid form and increases the visible light absorption range[19] (See ESI). In samples coupled with N,N-dimethylaniline, the increase of pH transformed the sample from deep red to yellow, this can be explained due to the similar structure to methyl orange, which also changes its colour from red to yellow. In the case of the diphenylamine coupled sample, similar behaviour was observed with pH, changing the colour of the samples from deep violet to light yellow. Samples coupled with naphtols are in an azo-hydrazone tautomeric equilibrium but independent of pH, they are only influenced by the polarity of the solvent used for washing samples, acetic acid and acetone (See ESI for Raman spectra and chemical species involved in equilibrium).

Table–1 – Specific surface area, energy gap from Tauc plot and methylene blue degradation performance. *Calculated from BET theory.

Sample	Specific Surface Area (m^2/g)[*]	Energy Gap (eV)	Methylene Blue degradation (%)
TiO2	45	3.25	100
UiO-66	563	3.70	42
UiO-66-NH2	566	2.87	63
N,N-dimethylaniline	816	1.89	75
1-naphtol	364	1.94	58
2-naphtol	359	2.00	4
Diphenylamine	451	1.71	91

The diazo-coupled reaction allows us to extend the absorption range of the bare MOF. After the reaction, we obtained a colour palette indicating that diazo coupling was successful (see ESI). In order to determine the absorption band-gap, diffuse reflectance spectrums of all specimens were measured (Fig. 3). The UiO-66 sample presents no absorption in the whole visible range, while UiO-66-NH$_2$ shows a shoulder at 400nm, which disappears at 450nm. The samples coupled with 1-naphtol and 2-naphtol exhibit similar spectra and a maximum absorption peak at 500nm with a tail up to 600nm. The N,N-dimethylaniline sample has an even more extended spectra, but with a maximum absorption peak at 550nm. The diphenylamine modified sample has a panchromatic coverage of the visible spectra, with a broad constant absorption peak up to 700nm. The red shift of the absorption spectra is in agreement with predictions from the particle in a box model, longer boxes indicate a larger red shift in the absorption spectra.
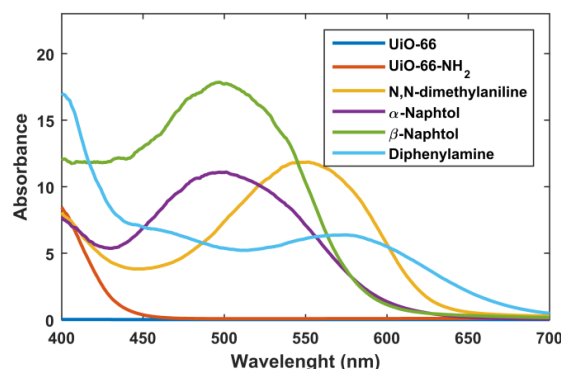

Fig 2 – Diffuse reflectance spectra for UiO-66, UiO-66-NH$_2$ and UiO-66-NH$_2$ diazo coupled samples. UiO-66 sample (blue line) does not exhibit light absorbance in the reported range.

To better show the red shift in the absorption spectra, the data was transformed into Tauc plots assuming direct allowed transitions (Table 1). The results of the transformation indicate that the absorption onset of the diphenylamine modified MOF is close to the minimum band gap for successful water splitting at pH=0, 1.23eV.

One direct and simple test of photocatalytic activity is the degradation of pollutants[20]. Nasalevich et al. showed the oxidation of benzaldehyde with a diazo modified MIL-125(Ti)-NH$_2$[11], while Wang et al[21]. and Liang et al[22] tested the performance on Cr(IV) reduction with MIL-125(Ti) and MIL-68(In)-NH$_2$ respectively. Laurier et al. observed the degradation of organic dyes, Rhodamine 6G, with Fe-based MOFs[23]. In our case, to prove the photocatalytic properties of the solids, the degradation of methylene blue in aqueous solution was performed (see ESI for experimental details). The degradation performance is correlated with the shift in the absorption edge of the MOFs (Fig SI-6). The only disagreement with this tendency is found in 1-naphthol and 2-naphthol coupled samples, this observation can by due to their low specific area (see Table 1)
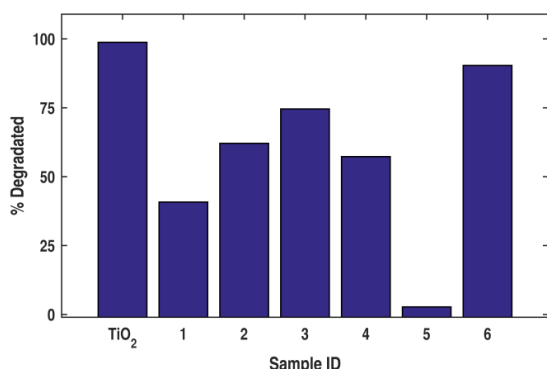
Fig 3 – Photocatalytic performance of coupled and uncoupled samples respect to TiO_2. Samples ID: 1) UiO-66, 2)UiO-66-NH2, 3)N,N-dimethylaniline, 4) 1-naphtol, 5) 2-naphtol, 6)Diphenylamine.

This work proves the modification of the absorption spectrum of UiO-66 MOF by covalent modification covering the whole visible spectrum. Covalent modification was performed via a diazo coupling of MOFs with amino substituted ligands and other molecules of limited size. It was observed that molecules with more than two aromatic rings did not react successfully under MOF-postfunctionalization conditions due to pore size exclusion. Diffusion through the pores was reduced by the functionalization, leaving a core of unreacted MOF coated with a functionalized shell. The covalent modification left the structure intact, maintaining its XRD pattern. This work shows that a judicious selection of coupling molecules produces significant modifications in the absorption spectra and that panchromaticity can be achieved. The good photocatalytic properties shown in pollutant degradation suggest the potentiality of these materials in the field of dye sensitized solar cells and water splitting.

Notes and references

1   M. O'Keeffe and O. M. Yaghi, *Chem. Rev.*, 2012, **112**, 675–702.
2   S. S. Kaye, A. Dailly, O. M. Yaghi and J. R. Long, *J. Am. Chem. Soc.*, 2007, **129**, 14176–14177.
3   C. G. Silva, A. Corma and H. García, *J. Mater. Chem.*, 2010, **20**, 3141.
4   M. Alvaro, E. Carbonell, B. Ferrer, F. X. Llabrés i Xamena and H. Garcia, *Chem. – Eur. J.*, 2007, **13**, 5106–5112.
5   B. O'Regan and M. Grätzel, *Nature*, 1991, **353**, 737–740.
6   J.-H. Yum, E. Baranoff, S. Wenger, M. K. Nazeeruddin and M. Grätzel, *Energy Environ. Sci.*, 2011, **4**, 842–857.
7   D. P. Hagberg, T. Edvinsson, T. Marinado, G. Boschloo, A. Hagfeldt and L. Sun, *Chem. Commun.*, 2006, **21**, 2245-2247..
8   A. Mishra, M. K. R. Fischer and P. Bäuerle, *Angew. Chem. Int. Ed. Engl.*, 2009, **48**, 2474–2499.
9   A. D. Burrows, C. G. Frost, M. F. Mahon and C. Richardson, *Angew. Chem. Int. Ed. Engl.*, 2008, **47** (**44**), 8482-8486.
10 D. Jiang, L. L. Keenan, A. D. Burrows and K. J. Edler, *Chem. Commun.,* 2012, **48**, 12053-12055.
11 M. A. Nasalevich, M. G. Goesten, T.J. Savenije, F. Kapteijn and J. Gascon, *Chem. Commun.*, 2013, **49**, 10575-10577.
12 J. Aguilera-Sigalat and D. Bradshaw, *Chem. Commun.*, 2014, **50**, 4711-4713.
13 J. H. Cavka, S. Jakobsen, U. Olsbye, N. Guillou, C. Lamberti, S. Bordiga and K. P. Lillerud, *J. Am. Chem. Soc.*, 2008, **130**, 13850–13851.
14 S. Jakobsen, D. Gianolio, D. S. Wragg, M. H. Nilsen, H. Emerich, S. Bordiga, C. Lamberti, U. Olsbye, M. Tilset and K. P. Lillerud, *Phys. Rev. B*, 2012, **86**, 125429.
15 S. Chavan, J. G. Vitillo, D. Gianolio, O. Zavorotynska, B. Civalleri, S. Jakobsen, M. H. Nilsen, L. Valenzano, C. Lamberti, K. P. Lillerud and S. Bordiga, *Phys. Chem. Chem. Phys.*, 2012, **14**, 1614–1626.
16 A. Schaate, P. Roy, A. Godt, J. Lippke, F, Waltz, M. Wiebcke and P. Behrens, *Chem.- Eur. J.*, 2011, **24**, 6643-6651.
17 M. Kandiah, S. Usseglio, S. Svelle, U. Olsbye, K. P. Lillerud and M. Tilset, *J. Mater. Chem.*, 2010, **20**, 9848-9851.
18 M. A. Rauf, S. Hisaindee and N. Saleh, *RSC Adv.¸* 2015, **5**, 18097-18110.
19 A. G. Gilani, M. Moghadam, M. S. Zakerhamidi and E. Moradi, *Dyes Pigm.,* 2011, **91 (2)**, 170-176.
20 C. C. Wang, J. R. Li, X, L. Lv, Y. Q. Zhang and G. Guo, *Energy Environ. Sci.,* 2014, **7**, 2831-2867.
21 H. Wang, X. Yuan, Y. Wu, G. Zeng, X. Chen, L. Leng, Z. Wu, L. Jiang and H. Li, *J. Hazard Mater.*, 2015, **286**, 187-194.
22 R. Liang, J. Shen, F. Jing and L. Wu, *Appl. Catal., B,* **162**, 245-251.
23 K. G. M. Lauriert, F. Vermoortele, R. Ameloot, D. E. De Vos, J. Hofkens and M. B.J Roeffaers, *J. Am. Chem. Soc.,* 2013, **135 (39)**, 14488-14491.